International Journal of Advanced Research in Chemical Science (IJARCS)
Volume 2, Issue 8, August 2015, PP 1-9
ISSN 2349-039X (Print) & ISSN 2349-0403 (Online)
www.arcjournals.org

The Simple and General-Base Catalyzed Aqueous Hydrolyses of Propionic and Butyric Anhydride

Floyd L. Wiseman, William C. Cooper, Curtis Heishman, Brandon Robinson

Abstract: *This article presents results of the aqueous hydrolyses of propionic and butyric anhydride between 0 and 60 ℃ in mildly acidic solutions of varying propanoate and butanoateconcentrations, respectively. These studies focus specifically on the temperature effectsand analysis of the activation parameters. The primary goal of this work is to establish mechanistic trends for simple and general-base catalyzed hydrolysis of smaller anhydrides, and to reevaluate conventional conclusions on certain modeling features. Resultsstrongly support a two-step mechanism for simple hydrolysisbelow room temperature,and a single-step mechanism for propanoate- and butanoate-catalyzed hydrolysis for all temperatures.Implications of these results and comparison with acetic anhydride hydrolysis are discussed.*

Keywords: *aqueous hydrolysis, Eyring plots, kinetics, pH technique, activation parameters, acetic, propionic, and butyric anhydride*

1. INTRODUCTION

This study, which complements historicaland recent work on the aqueous hydrolysis of acetic anhydride[1-16],includes analyses of the activation parameters for simple and general base-catalyzed hydrolyses of propionic and butyric anhydride. To the authors' knowledge, with the exception of the simple hydrolysis of propionic anhydride, data for these reactions hasnot been published in refereed scientific literature until now. Some work has been done in aqueous/organic mixtures [17], and in aquatic systems in the study of abiotic degradation [18]. More work probably has not been done with butyric anhydride due to its very low water solubility. Fortunately, the pH technique [2] lends itself to very low concentrations of reacting substrate, and has been used successfully in this work for studying the aqueous hydrolyses of propionic and butyric anhydride. Results of this study show that hydrolysis for both pathways appears to be mechanistically similar to acetic anhydride hydrolysis. For these anhydrides, curvature in the Eyring plots occurs only for simple hydrolysis, and then only at lower temperatures. There is no discernible curvature in the Eyring plots for general-base catalyzed hydrolysis, suggestingthe activation heat capacity term, which induces curvature at any temperature range, is insignificant. Researchers have traditionally invoked the heat capacity termto explain curvature in the Eyring plots for a variety of hydrolysis reactions[19, 20],but this work suggests the curvature is *not* due to this term.

The ratio of the rate constants for general base-catalyzed to simple hydrolysis varies from ~80 at 5°C to ~140 at 60°C for propionic anhydride, and from ~80 at 5 °C to~230 at 55 °C for butyric anhydride. Since the activation enthalpy is significantly *larger* for the catalyzed pathway for both anhydrides, the higher hydrolysis ratesarethe result of a less unfavorable activation entropy. This is likely due to less structural restrictions on the solvent moleculesfor the catalyzed pathway.

2. THEORY

2.1. The Mechanisms

The reaction for the simple single-stepmechanism for a symmetric anhydride is:

$$(RCO)_2O + (n+1)H_2O + B \rightarrow 2RCO_2H + B + nH_2O \quad (1)$$

in which $(n+1)H_2O$ represents the solvent shell consisting of n+1 water molecules, and B is either anotherwater molecule (simple hydrolysis) or a weak base (general-base catalysis – for this work the propanoate and butanoateions). Themolecularity of this reaction is open for debate; however, it is certain the reaction is at least termolecular (n = 0 for termolecular). The reversible, two-step steady-state mechanism is:

$$(RCO)_2O + (n+1)H_2O + B \underset{k_{-1}}{\overset{k_1}{\rightleftharpoons}} [RCO_2CO(OH)R^-, HB^+] + nH_2O$$

$$[RCO_2CO(OH)R^-, HB^+] + mH_2O \xrightarrow{K_2} 2RCO_2H + B + mH_2O \quad (2)$$

In which the subscript "1" refers to the formation of anion-pair tetrahedral intermediate, $[RCO_2CO(OH)R^-,HB^+]$, "−1" to the breakdown of the intermediateback to reactants, and "2" to the breakdown of the intermediate to products. It is noted here that the suggestion of an ion pair intermediate and solvent shells represented by $(n+1)H_2O$ and mH_2O are points of departure from the first paper in this series [2]. As will be discussed later, even if n and m are equal, it is likely that the respective solvent shells are structurally different. Furthermore, the number of solvent shell molecules is expected to depend upon B and the nature of the solvent medium. Application of the steady-state approximation to the ion-pair intermediate leads to the following expression for the rate constant:

$$k = \frac{k_1}{1+\alpha} \quad (3)$$

in which $\alpha = \frac{k_{-1}[H_2O]^{n-m}}{k_2}$. In this work general nucleophilic catalysis is not an issue since the buffer solutions were made using the same carboxylate ionas the product from the anhydride hydrolysis.

2.2. The General Rate Law

For either pathway represented by Reactions (1) and (2), the rate law is pseudo first-order, i.e.:

$$[(RCO)_2O] = [(RCO)_2O]_0 e^{-kt} \quad (4)$$

in which $[(RCO)_2O]_0$ is the initial anhydride concentration and k here represents the experimentally observed rate constant.For systems in which simple hydrolysis and general-base catalyzed hydrolysis both occur, the observed rate constant is expressed as:

$$k = k_w[H_2O]^{n+2} + k_b[H_2O]^{n+1}[B] \quad (5)$$

in which "B"here represents the carboxylateion, "w" refers to simple hydrolysis, and "b" to general base-catalyzed hydrolysis. The form of the equation used in this work is:

$$k = k_w' + \phi k_b' \quad (6)$$

in which $\phi = \frac{[B]}{[H_2O]}$, $k_w' = k_w[H_2O]^{(n+2)}$, and $k_b' = k_b[H_2O]^{(n+2)}$.k_w' and k_b' are the experimental pseudo first-order rate constants for the respective pathways.Table 1 shows the overall rate constant expressions for all possiblesingle-step/two-step mechanism pairs.As suggested by Equation (6), and consistently verified in this work, k is linear with ϕ.

Table1.*Combined rate constant expressions for the single-step and two-step mechanisms. The subscript "w" signifies simple water hydrolysis; "b" signifiesgeneral base-catalyzed hydrolysis; "1" signifies the forward reaction forming the tetrahedral intermediate; "–1" signifies the reverse reaction back to the reactants; and "2" signifies the forward reaction for the intermediate forming the products. [B] is the concentration of the carboxylate ion*.

Pathway pair	Equation	Experimental rateconstant expression	Definition of terms
Single step (w)/ single step (b)	T1	$(k_w + \phi k_b)[H_2O]^{(n+2)}$	$\phi = \frac{[B]}{[H_2O]}$
Single step (w)/ two-step (b)	T2	$\left(k_w + \frac{\phi k_{b1}}{1+\alpha_b}\right)[H_2O]^{(n+2)}$	$\alpha_b = \frac{k_{b-1}[H_2O]^{n-m}}{k_{b2}}$
Single step (b)/ two step (w)	T3	$\left(\frac{k_{w1}}{1+\alpha_w} + \phi k_b\right)[H_2O]^{(n+2)}$	$\alpha_w = \frac{k_{w-1}[H_2O]^{n-m}}{k_{w2}}$
Two step (w)/ Two step (b)	T4	$\left(\frac{k_{w1}}{1+\alpha_w} + \frac{\phi k_{b1}}{1+\alpha_b}\right)[H_2O]^{(n+2)}$	

2.3. The Rate Law in Terms of the pH for a Buffered Solution

All the reactions in this work wereconducted in buffer solutions in which the concentrations of the carboxylate were much higher than the reactive anhydrides. Precision in replicate trials is generally better if the reactions are carried out in buffer solutions, probably because the buffer model has fewer regression parameters.The rate law in terms of the pH fora buffer solution isderived in Reference 1, and is:

$$\mathrm{pH} = \mathrm{pK_a} + \log\frac{a_-}{\gamma[\mathrm{RCO_2H}]_\infty} - \log\left(1 - \frac{2[(\mathrm{RCO})_2\mathrm{O}]_0 \mathrm{e}^{-\mathrm{kt}}}{[\mathrm{RCO_2H}]_\infty}\right) \tag{7}$$

in which K_a is the acid dissociation constant of the acid formed from the anhydride hydrolysis, a_- is the activity of the carboxylate ion, γ is the activity coefficient of the acid, $[\mathrm{RCO_2H}]_\infty$ is the acid concentration after hydrolysis is complete (time = ∞), and $[(\mathrm{RCO})_2\mathrm{O}]_0$ is the anhydride concentration when monitoring is initiated (time = 0). Equation (7) is a three-parameter model, for whichthe regression parameters are $\mathrm{pK_a} + \log\frac{a_-}{\gamma[\mathrm{RCO_2H}]_\infty}$, $\frac{2[(\mathrm{RCO})_2\mathrm{O}]_0}{[\mathrm{RCO_2H}]_\infty}$, and k.

2.4. The Eyring Expressions for the Elementary Rate Constants

The simple Eyring rate constantexpression is :

$$\mathrm{k} = \frac{\mathrm{k_B T}}{\mathrm{h}}\frac{\prod_{\mathrm{i}=1}^{\mathrm{o}}\gamma_\mathrm{i}}{\gamma^\ddagger}(M^{1-\mathrm{o}})\mathrm{e}^{\left[\Delta\mathrm{S}_\mathrm{r}^\ddagger - \frac{\Delta\mathrm{H}_\mathrm{r}^\ddagger}{\mathrm{T}} + \Delta\mathrm{C}_\mathrm{p}^\ddagger\left(\ln\frac{\mathrm{T}}{\mathrm{T_r}} + \frac{\mathrm{T_r}}{\mathrm{T}} - 1\right)\right]/\mathrm{R}} \tag{8}$$

in which k_B is Boltzmann's constant, h is Planck's constant, o is the molecularity,*M* is the molarity ($\mathrm{mol\cdot dm^{-3}}$), γ_i representsthe reactant-state activity coefficients, $\gamma^\ddagger$ is the transition structure activity coefficient, R is the gas constant,$\Delta H_r^\ddagger$ is the activation enthalpy, $\Delta S_r^\ddagger$ is the activation entropy, $\Delta C_p^\ddagger$ is the temperature-independent activation heat capacity, and the subscript "r" denotes a reference temperature.There is more diffuse charge distribution as the transition structure is formed, but there is no net change in the charge;so the term$\frac{\prod_{\mathrm{i}=1}^{\mathrm{o}}\gamma_\mathrm{i}}{\gamma^\ddagger}$ is assumed to be1. The kinetic parameters α_w and α_b appearing in Table 1 are given by the following Eyring form:

$$\alpha = \left(\frac{[\mathrm{H_2O}]}{M}\right)^{\mathrm{n-m}} \mathrm{e}^{\left[\frac{\Delta\Delta\mathrm{H}_\mathrm{r}^\ddagger}{\mathrm{T}} - \Delta\Delta\mathrm{S}_\mathrm{r}^\ddagger - \Delta\Delta\mathrm{C}_\mathrm{p}^\ddagger\left(\ln\frac{\mathrm{T}}{\mathrm{T_r}} + \frac{\mathrm{T_r}}{\mathrm{T}} - 1\right)\right]/\mathrm{R}}$$

$$= \left(\frac{[\mathrm{H_2O}]}{M}\right)^{\mathrm{n-m}} \mathrm{e}^{-\Delta\Delta\mathrm{S}_\mathrm{r}^\ddagger/\mathrm{R}}\mathrm{e}^{\left[\frac{\Delta\Delta\mathrm{H}_\mathrm{r}^\ddagger}{\mathrm{T}} - \Delta\Delta\mathrm{C}_\mathrm{p}^\ddagger\left(\ln\frac{\mathrm{T}}{\mathrm{T_r}} + \frac{\mathrm{T_r}}{\mathrm{T}} - 1\right)\right]/\mathrm{R}} \tag{9}$$

in which $\Delta\Delta H_r^\ddagger = \Delta H_{r,2}^\ddagger - \Delta H_{r.-1}^\ddagger$, $\Delta\Delta S_r^\ddagger = \Delta S_{r,2}^\ddagger - \Delta S_{r,-1}^\ddagger$, and $\Delta\Delta C_p^\ddagger = \Delta C_{p,2}^\ddagger - \Delta C_{p,-1}^\ddagger$. The full set of regression parameters for the αtermis$\Delta\Delta H_r^\ddagger$, $\Delta\Delta C_p^\ddagger$, and $\left(\frac{[\mathrm{H_2O}]}{M}\right)^{\mathrm{n-m}} \mathrm{e}^{-\Delta\Delta\mathrm{S}_\mathrm{r}^\ddagger/\mathrm{R}}$.However, in this work, $\Delta\Delta C_p^\ddagger$ is set to 0 and n and m are assumed to be equal. The practical significance of the α term is its ability to induce curvature in the Eyring plots at lower temperatures.

2.5. The Overall Rate Constant Expressions

Of the rate constant expressions in Table 1, Equations (T2) and (T4) can be immediately ruled outbecause the Eyring plots for general-base catalyzed hydrolysis do not show any discernible curvature over the temperature ranges studied in this work.

- *Rate Constant Expressions for Equation (T1) (single-step for both reaction pathways):*

The single-step rate constant has the general form $\mathrm{k}' = \frac{\mathrm{k_B T}}{\mathrm{h}}\left(\frac{[\mathrm{H_2O}]}{M}\right)^2 \mathrm{e}^{\left[\Delta\mathrm{S}_\mathrm{r}^\ddagger - \frac{\Delta\mathrm{H}_\mathrm{r}^\ddagger}{\mathrm{T}} + \Delta\mathrm{C}_\mathrm{p}^\ddagger\left(\ln\frac{\mathrm{T}}{\mathrm{T_r}} + \frac{\mathrm{T_r}}{\mathrm{T}} - 1\right)\right]/\mathrm{R}}$, assuming n = 0. More convenient formsfor the two pathways are:

$$\mathrm{R}\left\{\ln\frac{\mathrm{k_w' h}}{\mathrm{k_B T}} - 2\ln\left(\frac{[\mathrm{H_2O}]}{M}\right)\right\} = \Delta\mathrm{S}_\mathrm{w}^\ddagger - \frac{\Delta\mathrm{H}_\mathrm{w}^\ddagger}{\mathrm{T}} + \Delta\mathrm{C}_{\mathrm{p,w}}^\ddagger\left(\ln\frac{\mathrm{T}}{\mathrm{T_r}} + \frac{\mathrm{T_r}}{\mathrm{T}} - 1\right) \tag{10}$$

$$\mathrm{R}\left\{\ln\frac{\mathrm{k_b' h}}{\mathrm{k_B T}} - 2\ln\left(\frac{[\mathrm{H_2O}]}{M}\right)\right\} = \Delta\mathrm{S}_\mathrm{b}^\ddagger - \frac{\Delta\mathrm{H}_\mathrm{b}^\ddagger}{\mathrm{T}} + \Delta\mathrm{C}_{\mathrm{p,b}}^\ddagger\left(\ln\frac{\mathrm{T}}{\mathrm{T_r}} + \frac{\mathrm{T_r}}{\mathrm{T}} - 1\right) \tag{11}$$

in which the subscript "r" has been dropped for brevity. Regression analysis of the data plotted as $\mathrm{R}\left\{\ln\frac{\mathrm{k' h}}{\mathrm{k_B T}} - 2\ln\left(\frac{[\mathrm{H_2O}]}{M}\right)\right\}$ vs. $\mathrm{T^{-1}}$ directlyyields $\Delta S^\ddagger$ and $\Delta C_p^\ddagger$ in $\mathrm{J\cdot K^{-1}\cdot mol^{-1}}$, and $\Delta H^\ddagger$ in $\mathrm{J\cdot mol^{-1}}$.

- *Rate Constant Expressions for Equation (T3) (single-step for base-catalyzed hydrolysis and two-step for simple hydrolysis)*

The experimental data suggests this is the mechanism pair that actually occurs. Equation (11) is used for the base-catalyzed hydrolysis, except the $\Delta C_{p,b}^{\ddagger}$ term is excluded since the Eyring plots are linear. The two-step rate constant has the general form $k' = \frac{k_B T}{h(1+\alpha)} \left(\frac{[H_2O]}{M}\right)^2 e^{\left[\Delta S_r^{\ddagger} - \frac{\Delta H_r^{\ddagger}}{T} + \Delta C_p^{\ddagger}\left(\ln\frac{T}{T_r} + \frac{T_r}{T} - 1\right)\right]/R}$. Setting n = m = 0 and $\Delta C_{p,w}^{\ddagger} = 0$ yields the following form that is used in the regression analysis:

$$R\left\{\ln\frac{k_w' h}{k_B T} - 2\ln\left(\frac{[H_2O]}{M}\right)\right\} = \Delta S_{w1}^{\ddagger} - \frac{\Delta H_{w1}^{\ddagger}}{T} - R\ln\left\{1 + e^{\left(\frac{\Delta\Delta H_w^{\ddagger}}{T} - \Delta\Delta S_w^{\ddagger}\right)/R}\right\} \quad (12)$$

The regression parameters for Equation (12) are $\Delta S_{w1}^{\ddagger}$, $\Delta H_{w1}^{\ddagger}$, $\Delta\Delta H_w^{\ddagger}$, and $\Delta\Delta S_w^{\ddagger}$.

3. EXPERIMENTAL AND DATA ANALYSES

Propionic and butyric anhydride (Aldrich, ≥ 99%) were used as received. Reaction solutions for propionic anhydride were prepared using deionized water, sodium propanoate (Acros, 99.0 – 100.5%), a 2.0-mol·dm^{-3} solution of propanoic acid (Acros, 99+%, extra pure), and sodium chloride (Flinn Scientific, Inc.), which was used to adjust the ionic strength to 0.500 mol·dm^{-3}.Propanoate concentrations ranged from 0.0095 to 0.475 mol·dm^{-3}. Reaction solutions for butyric anhydride were prepared using deionized water, sodium butanoate (Acros, 99.0 – 100.5%), and sodium chloride, which was used to adjust the ionic strength to 0.201mol·dm^{-3}. Butyric acid was not used for these reaction solutions. Butanoate concentrations ranged from 0.0011 to 0.201 mol·dm^{-3}. The lower ionic strength for butyric anhydride was used because of its very low water solubility.

Temperatures were maintained at ±0.01°C using a water bath and a thermostatted water circulator (Thermo Scientific, Haake SC 100). Since the thermostat only heated the water, ice was used to maintain temperatures lower than room temperature. The water bath was placed on a magnetic stirrer to allow the reaction solutions to becontinuously stirred. The reaction time was monitored manually using a digital timer, and the pH, which ranged between 4 and 5.5, was monitored using an AccumetModel 15 pH meter set to read to 0.001 pH unit and equipped with atemperature probe and a Thermo Scientific Orion Ross pH electrode. The electrode was periodically calibrated using standard pH 7.00, 5.00, 4.00, and 3.00 buffer solutions (Fisher Scientific) as appropriate.As evidenced by the quality of the regression analyses, the experimental rate constants did not appear to be pH-dependent within this pH range.

All propanoate reaction solutions had a density of 1.020 (0.002) g·cm^{-3}at room temperature, and all butanoate reaction solutions had a density of 1.008 (0.001) g·cm^{-3}. The water concentration for all reaction solutions was 55.0 (0.3) mol·dm^{-3}. For each trial a few drops of the anhydride, commensurate with the carboxylate concentrations, were added to ~100mL of the reaction solution. Fewer drops were used for the butyric anhydride system, again because of the solubility issues. Reaction monitoring began when the change in pH was less than ~0.1 pH unit per minute. At least four trials were conducted for each reaction solution, and the precision errors for multiple trials were generally within 1.5%.The change in pH ranged from ~0.15 pH unit for the faster reactions at the higher temperatures to ~0.8 pH unit for the slower reactions at the lower temperatures. The number of data points ranged from 15 for the faster reactions to 40 for the slower reactions.

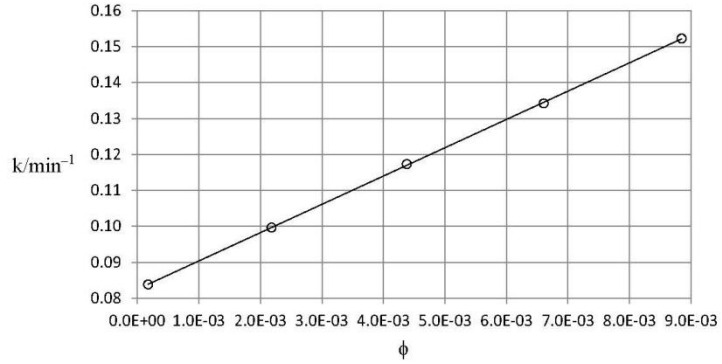

Figure1.*Typical data set (k vs. ϕ) showing the linear regression analysis of Equation (6). Results for this particular data set for the propionic anhydride system at 25.0 °C are:* $k_w' = 0.0825\ min^{-1}$, $k_b' = 7.872\ min^{-1}$.

The raw kinetic data (as pH vs. time) was analyzed using Equation (7). All data points were weighted equally in the regression analyses. The correlation coefficients generally ranged from 0.99995 for the faster reactions to 0.99999 for the intermediate and slower reactions. The resultant kinetic data at each temperature was then analyzed using Equation (6). Figure 1 shows a typical data set (k vs. ϕ) with the regression line. Finally, the data sets for k_w' and k_b' were analyzed using Equations (11) and (12) to obtain the activation parameters for the suite of mechanisms.

4. RESULTS AND DISCUSSION

4.1. Regression Analyses

Figure 2 shows plots of $R\left\{\ln\frac{k_w' h}{k_B T} - 2\ln\left(\frac{[H_2O]}{M}\right)\right\}$ vs. T^{-1} from the regression analysis of Equation (12) for the simple hydrolysis of acetic, propionic, and butyric anhydride. Figure 3 shows plots of $R\left\{\ln\frac{k_b' h}{k_B T} - 2\ln\left(\frac{[H_2O]}{M}\right)\right\}$ vs. T^{-1} from the regression analysis of Equation (11) for the general base-catalyzed hydrolysis of acetic, propionic, and butyric anhydride. Table 2 shows the activation parameters from theseregression analyses. Reference 2 discusses the statistic "F" tests for the simple and the general-base catalyzed hydrolyses modelsfor acetic anhydride. Since propionic and butyric anhydride exhibit nearly identical behavior, the statistical conclusions from Reference 2are assumed to apply here as well. For this reason, other modeling options have not been explored. Figure 4 shows plots of α vs. T (from 270 to 300 K) for all three anhydrides.

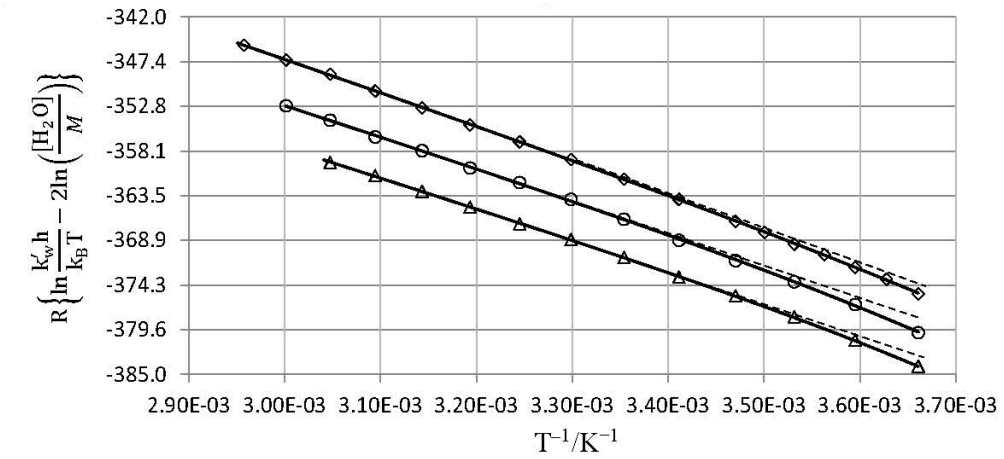

Figure2.*Plots of data as* $R\left\{ln\frac{k_w' h}{k_B T} - 2ln\left(\frac{[H_2O]}{M}\right)\right\}$ *vs.* T^{-1} *and the regression analysis of the data using Equation (12) for all three anhydrides (◇= acetic anhydride, o = propionic anhydride, △ = butyric anhydride). Data for acetic anhydride is from Reference 2. Dashed lines are included here to highlight the curvature at lower temperatures.*

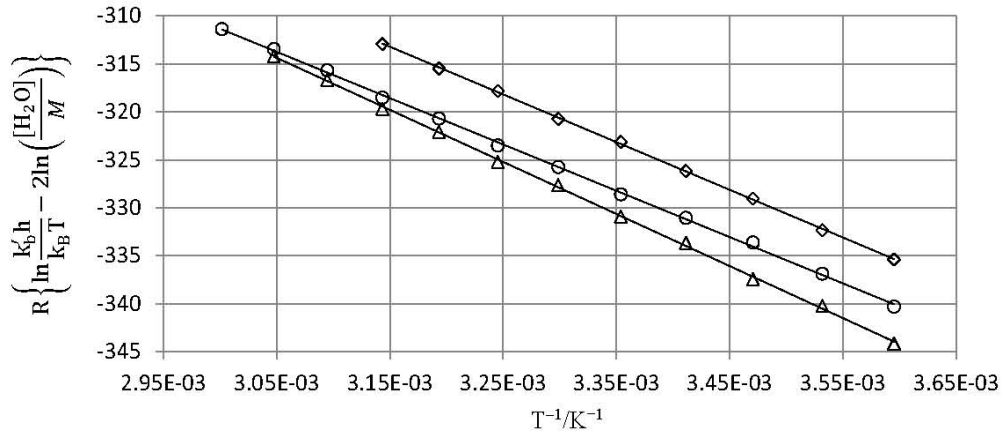

Figure3.*Plots of* $R\left\{ln\frac{k_b^{'}h}{k_BT}-2ln\left(\frac{[H_2O]}{M}\right)\right\}$ *vs.* T^{-1} *and the regression analysis of the data using Equation (11)(excluding the activation heat capacity term) for all three anhydrides (◇= acetic anhydride,* o *= propionic anhydride,* △*= butyric anhydride). Data for acetic anhydride is from Reference 2.*

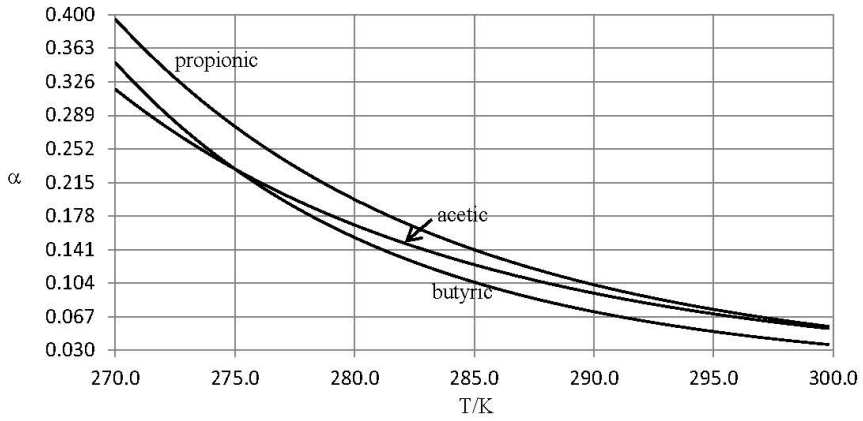

Figure4.*Plots of* α *vs.* $T(\Delta\Delta C_p^{\ddagger}=0$ *and* $n = m)$ *for the simple hydrolysis of acetic, propionic, and butyric anhydride.*

Table2.*Results of regression analyses of the data using Equations (11) and (12), with the activation heat capacity terms set to zero. The estimated errors from the regression analyses are in parentheses. For the analysis using Equation (12), n and m are assumed to be 0. The ionic strength for the hydrolysis of acetic and propionic anhydride is 0.500 mol·dm*$^{-3}$*; and for butyric anhydride it is 0.201mol·dm*$^{-3}$*.The corresponding Eyring plots are shown in Figures 2 and 3.*

Type of reaction	Anhydride	$\Delta H^{\ddagger}$/kJ·mol^{-1}	$\Delta S^{\ddagger}$/J·K^{-1}·mol^{-1}	$\Delta\Delta H^{\ddagger}$/kJ·mol^{-1}	$\Delta\Delta S^{\ddagger}$/J·K^{-1}·mol^{-1}
Simple hydrolysis	Acetic	39.5 (0.8)	−229 (2)	37 (10)	145 (39)
	Propionic	37.3 (1.6)	−241 (5)	44 (19)	169 (71)
	Butyric	36.6 (0.7)	−248 (2)	51 (11)	198 (43)
General-base catalyzed hydrolysis	Acetic	49.7 (0.3)	−157 (1)	·····	·····
	Propionic	48.3 (0.4)	−167 (1)	·····	·····
	Butyric	54.9 (0.5)	−147 (2)	·····	·····

4.2. Comparison with other Work and Unique Contributions of this Work

The value for $\Delta H_w^{\ddagger}$ for propionic anhydride is somewhat low comparedwith other literature values (e.g. 39.8 kJ·mol^{-1} [21] and 40.8 kJ·mol^{-1} [22]). However, the value in this work is expected to be slightly different due to the inclusion of the α term in the model.The value for $\Delta S_w^{\ddagger}$ is high compared to other literature values (e.g. −167 J·K^{-1}·mol^{-1} [21]and −162 J·K^{-1}·mol^{-1} [22]), but this difference is due to the term $2R\ln\left(\frac{[H_2O]}{M}\right)$, which offsets the valuesin this work by −67 J·K^{-1}·mol^{-1}.It is noted here that this term depends upon the presumed molecularity of the water molecules. In general, values for $\Delta S_w^{\ddagger}$ are offset by the factor $(n+2)R\ln\left(\frac{[H_2O]}{M}\right)$.In fact, very large negative values are possible if the solvent shells contributing to the molecularity are large.

Work by Isaacs and Hoffman [18] on the aqueous abiotic degradation of butyric anhydride shows a half-life of 17 to 18 minutes at 22 °C and a pH around 4. This is in excellent agreement with this work. Their work also shows a noticeable increase of the degradation rates at pH levels of 7 and higher. Studies here did not extend to these higher pH levels, but it is likely that these higher rates indicate hydroxide-ion catalysis.

One major contribution of this work, along with previous workin this series [2], is the separate analyses for simple and general-base catalyzed hydrolysis. Secondly, this work applies the α term as an alternative modelling feature to account for the low-temperature curvature in the Eyring plots for simple hydrolysis. Several reasons favor use of the α term over the activation heat capacity term. For one, values quoted in the literature for the activation heat capacity for some systems seem unreasonably large. Secondly, the α term favors curvature at lower temperatures, a feature that is consistently seen in the systems studied in this series. Finally, it seems plausible that a significant activation heat capacity term should show curvature in the Eyring plots for both mechanisms, but the

plots for general-base catalysis show no discernible curvature over the temperature ranges studied. While the results of this work do not prove the mechanism depicted by Reaction (2), it certainly suggests the need for a paradigm shift away from the conventional thought.One final, but noteworthy contribution of this work is the first-time analysis (to the authors' knowledge) for the aqueous hydrolysis of butyric anhydride under variable-temperature conditions.

4.3. Mechanistic Implicationsfor Simple Water Hydrolysis

Values for $\Delta\Delta H_w^{\ddagger}$ are positive for all three anhydrides, suggestinga much higher energy requirement for the decomposition of the intermediates to the product state. This suggeststhat upon formation, the ion-pair intermediate is structurally poised for return to the reactantstate. Some solvent structural reorganization is likely required to poise the intermediate for reaction to products. The positive values for $\Delta\Delta S_w^{\ddagger}$ certainlysupport this, and further suggests that the solvent shell may consist of several water molecules. Again it should be noted that values for $\Delta\Delta S_w^{\ddagger}$ depend upon the presumed water molecularities of the forward (k_2) and reverse (k_{-1}) steps. If the reversible formation of the tetrahedral intermediate is the correct mechanism, as suggested by Bunton, Fuller, Perry, and Shiner[23], then this work shows the return to the reactantstate is thermodynamically favoredonly at lower temperatures where the $\Delta\Delta H_w^{\ddagger}$term is dominant. Conversely, the positive values for $\Delta\Delta S_w^{\ddagger}$drive the intermediate to the product state at higher temperatures. In effect, the reversible, two-step mechanism becomes a one-step mechanism as the temperature increases.

The lower temperature range (below room temperature) is the region where the mechanism begins to shift from one-step to two-step. However, given that the values for α are still less than 1 at 0 °C, the mechanism is not firmly two-stepeven at this temperature. In any regard, solvent changes within this range may have significant or unusual effects upon the rate constants. In fact, studies of the hydrolysis of propionic anhydride in water/deuterium oxide mixtures show a fairly large normal kinetic solvent isotope effect, from ~2.7 to ~3.2,in this temperature range. A minimum occurs at ~30 °C[24].Davis and Hogg have shown that this large isotope effect is due to the effect upon the activation entropy[22]. The activation enthalpy actually has a slight inverse isotope effect. Kinetic solvent isotope effects are comparable for acetic anhydride, where a maximum occurs at ~15 °C[24]. The isotope effect for acetic anhydride falls rapidly above 25 °C, which may correlate with the fact that αisinsignificant above this temperature.

4.4. Mechanistic Implications for General Base-Catalyzed Hydrolysis

Two noteworthy points can be made about the general base-catalyzed hydrolysis. First, the fact that catalyzed hydrolysis is faster than simple hydrolysis is due exclusively to a much less demanding entropic term, which overrides the higher energy demand for this pathway. This effect becomes more pronounced at higher temperatures, and suggests there may be less structural assistance required from the solvent shell for general-base catalysis.The second point, one that runs counter to conventional thought and that bears repeating here, is the activation heat capacity is statistically insignificant. Of course, this term isnot expected to be exactly zero, but it must in fact be numerically large to render any noticeable curvature. The reason is the functional part of thisterm (i.e. $\ln\frac{T}{T_r}+\frac{T_r}{T}-1$) is rather insensitive to temperature. In addition to sometimes being unreasonably large,as previously mentioned, the activation heat capacity termcannot adequately account for the curvaturein some systems [25].

4.5. Correlation of Molecular Size with the Activation Parameters

Figure 5 shows plots of the activation parameters vs. the number of carbon atoms for the three anhydrides and for both pathways. For simple hydrolysis, the activation enthalpy appears to become slightly smaller with increasing number of carbon atoms. However, this conclusion is tenuous as the errors are relatively large for this parameter. On the other hand, the activation entropy definitely becomes more negative with increasing size. The smaller energy demand for the formation of the tetrahedral intermediate for the larger anhydrides may be due to inductive effects. The larger negative activation entropies are probably due to larger solvent shells required to stabilize the larger core transition structures. For base-catalyzed hydrolysis, butyric anhydride does not follow the same trend

for either activation parameter. The much higher energy demand for butyric anhydride may be due to a stronger steric hindrance as the butanoate diffuses in proximity to the anhydride to facilitate the attacking water molecule. This higher energy demand may in turn reduce the energy requirement for a stringently restructured solvent shell. This notion is implied by the noticeably smaller negative activation entropy.

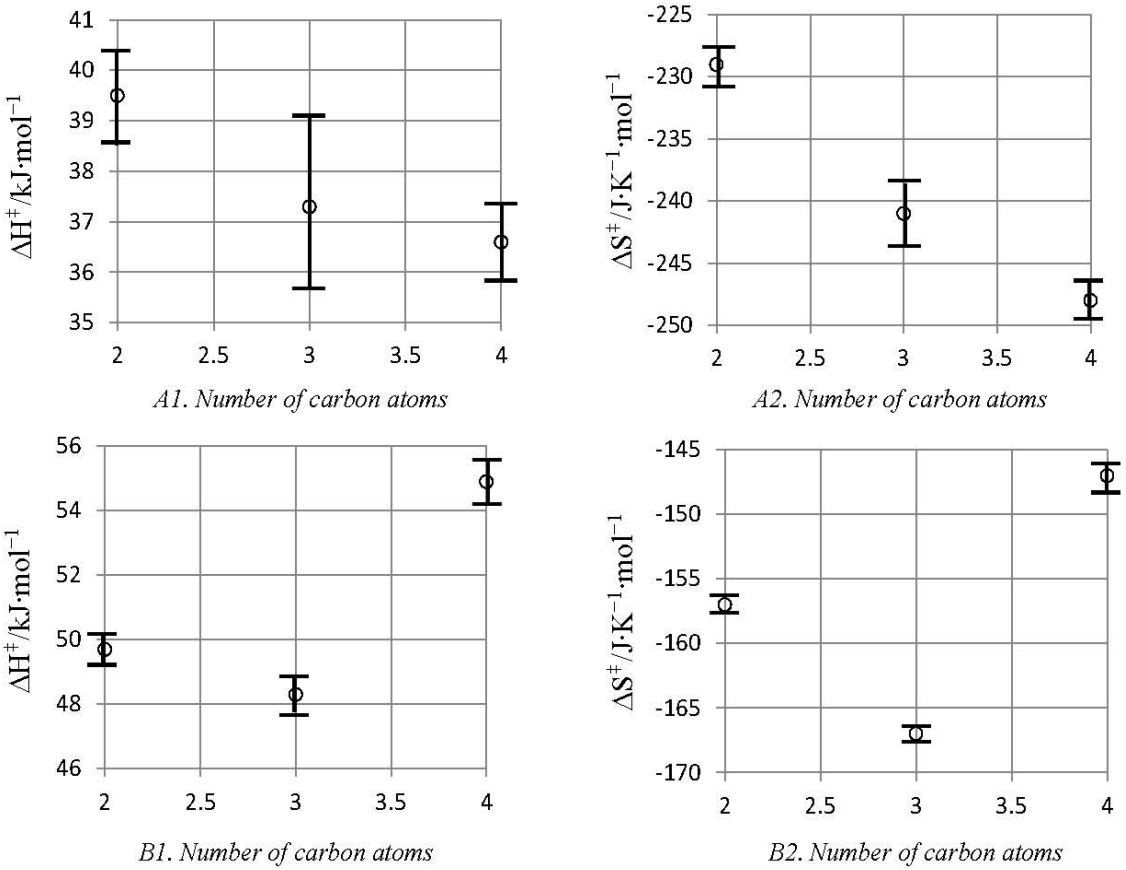

Figure5. *Plots of the activation parameters vs. the number of carbon atoms (with error bars) for the anhydrides studied in this work (A1 and A2 − simple hydrolysis; B1 and B2 – general base-catalyzed hydrolysis).*

5. CONCLUSIONS

This work has clearly established trends for the smaller anhydrides. But a continuation of this work for larger anhydrides, particularly those that exhibit noticeable curvature in the Eyring plots, would be beneficial for further establishing trends. Conducting studies in which the catalytic carboxylate ion is structurally different than the anhydride may also prove useful, as would further explorations of sterically-hindered catalytic systems. Finally, conducting proton inventory analyses would bebeneficial for establishing trends in the detailed nature of the transition structures, particularly regarding the number and type of protons involved in the transition structure.

REFERENCES

[1] N. A. Amenaghawon, E. I. Osagie, S. O. Osemwengie, S. E. Ogbeide, C. O. Okieiman, *Nigerian J. Tech.*, **2013**;*32* (3), 386 – 392.

[2] F. L. Wiseman, *J. Phys. Org. Chem.*, **2012**;*65*, 1105 – 1111.

[3] W. H. Hirota, R. B. Rodrigues, C. Sayer, R. do Giudici, *Chem. Eng. Sci.*, **2010**, *65* (12), 3849 − 3858.

[4] K. J. P. Orton, M. Jones, *J. Chem. Soc.*, **1912**, *101*, 1708 – 1720.

[5] F. A. Cleland, R. H. Wilhelm, *AlChE J.*, **1956**, *2*, 489.

[6] V. Gold, *Trans. Far. Soc.*, **1948**, *44*, 506 – 518.

[7] T. L. Smith, *J. Phys. Chem.*, **1955**, *59* (5), 385 – 388.

[8] H. J. Janssen, C. H. Haydel, L. H. Greathouse, *Ind. Eng. Chem.*, **1957**, *49* (2), 197 – 201.

[9] D. Glasser, D. F. Williams, *Ind. Eng. Chem. Fund.*, **1971**, *10* (3), 516 – 519.
[10] A.C. D. Rivett, N. V. Sidgwick, *J. Chem. Soc.*, **1910**, *97*, 732 – 741.
[11] K. Kralj, *Ind. Eng. Chem.*, **2007**, *13* (4), 631 – 636.
[12] W. C. Bell, K. S. Booksh, M. L. Myrick, *Anal. Chem.*, **1998**, *70* (2), 332 – 339.
[13] S. Haji, C. Erkey, *Chem. Eng. Ed.*, **2005**, *39* (1), 56 – 61.
[14] S. P. Asprey, B. W. Wojceichowski, N. M. Rice, A. Dorcas, *Chem. Eng. Sci.*, **1996**, *51* (20), 4681 – 4692.
[15] A. Zogg, U. Fischer, K. Hungerbuhler, *Chemom. Int. Lab. Sys.*, **2004**, *71* (2), 165 – 176.
[16] G. Puxty, M. Meader, R. R. Rhinehart, S. Alam, S. Moore, P. J. Gemperline, *J. Chemom.*, **2005**, *19*, 329 – 340.
[17] J. B. Conn, G. B. Kistiakowsky, R. M. Roberts, E. A. Smith, *J. Am. Chem. Soc.*, **1942**, *64* (8), 1747 – 1752.
[18] Isaacs, C. M. Hoffman, "n-Butyric Anhydride – Abiotic Biodegradation: Hydrolysis", Final Report #1204-HYD, **2002**, Eastman Kodak Company.
[19] R. E. Robertson, B. Rossall, W. A. Redmond, *Can. J. Chem.*, **1971**; *49*, 3665 – 3670.
[20] Batts, V. J. Gold, *J. Chem. Soc.*, **1969**; 984 – 987.
[21] S. L. Johnson, *Adv. Phys. Org. Chem.*, **1967**; *5*, 237.
[22] K. R. Davis, J. L. Hogg, *J. Org. Chem.*, **1983**; *48*, 1041 – 1047.
[23] A. Bunton, N. A. Fuller, S. G. Perry, V. J. Shiner, *J. Chem. Soc.*, **1963**; 2918 – 2926.
[24] B. Rossall, R. E. Robertson, *Can. J. Chem.*, **1975**; *53*, 869 – 877.
[25] M. J. Blandamer, J. Burgess, N. P. Clare, P. P. Duce, R. P. Gray, R. E. Robertson, J. W. M. Scott, *J. Chem. Soc., Faraday Trans. 1*, **1982**, *78*, 1103 – 1115.

Authors' Biography

Dr. Floyd Wiseman, Since retiring from the United States Air Force, Dr. Wiseman has spent his post-retirement career working at a software company developing atmospheric reactivity models, and as an instructor and assistant professor at various academic institutions in the eastern United States. While at the company, Dr. Wiseman developed the theory outlining configuration-specific kinetic molecular theory (Wiseman, F. L.; "Configuration-Specific Kinetic Molecular Theory Applied to an Ideal Binary Gas Mixture"; *J. Phys. Chem. A*; **2006**; *110*; 11377; Wiseman, F. L.; "Configuration-Specific Kinetic Molecular Theory Applied to the Elastic Collisions of Hard Spherical Molecules"; *J. Phys. Chem. A*; **2006**; *110*; 6379). In addition, Dr. Wiseman has successfully pioneered the use of pH techniques for studying a variety of aqueous hydrolyses reactions (Wiseman, F. L.; "New Insight on an Old Reaction – the Aqueous Hydrolysis of Acetic Anhydride"; *J. Phys. Org. Chem.*; **2012**; *25*; 1105; Wiseman, F. L.; "Monitoring the Rate of Solvolytic Decomposition of Benzenediazonium Tetrafluoroborate in Aqueous Media Using a pH Electrode"; *J. Chem. Ed.*; **2005**; *82*; 1841). Dr. Wiseman is currently assistant professor of chemistry at Davis and Elkins College in West Virginia, USA.

Dr. Cooper, completed his Ph.D. degree at the University of South Carolina under Drs. Bruce Dunlap and Jerome Odom. There he studied the catalytic role the Met Loop of DihydrofolateReductase. He went on to complete a postdoctoral position under Dr. Trevor M. Penning at the University of Pennsylvania. He studied the steady-state and transient state kinetics of the 3a-Hydroxysteroid Dehydrogenase mechanism. In this study, he solved all enzymatic complexes present as well as all rate constants in this mechanism which resulted in the publication: William C. Cooper, Yi Jin, and Trevor M. Penning, (2007) Elucidation of a Complete KineticMechanism for a Mammalian Hydroxysteroid Dehydrogenase (HSD) and Identificationof All Enzyme Forms on the Reaction Coordinate, the Example of Rat Liver 3alpha-HSD (AKR1C9), Journal of Biological Chemistry, 282, 33484-33493.

He has moved on to Eastern New Mexico University where he is an Assistant Professor of Chemistry in the Department of Physical Sciences. Here he has submitted the manuscript for publication in the Journal of Organic Chemistry (ACS):A Comparative Study on the Hydrolysis of Acetic Anhydride and N,N-Dimethyl Formamide: Kinetic Isotope Effect, Transition-State Structure, Polarity and Solvent Effect:William C. Cooper, Abhinay Chikuloorie, Suhesh Polam, Floyd Wiseman, and Dane Scott, Journal of Organic Chemistry (ACS).